DOI 10.24425/aee.2025.154985

Optimization of supercapacitor energy storage systems and solar power systems integrated into urban railway lines to lessen CO_2 emissions

VAN KHOI TRAN ✉, THI HOAI THU ANH AN

Faculty of Electrical – Electronic Engineering, University of Transport and Communications
No.3 Cau Giay Street, Lang Thuong Ward, Dong Da District, Hanoi, Vietnam
e-mail: {✉ tvkhoi.ktd/htanh.ktd}@utc.edu.vn

(Received: 07.02.2025, revised: 14.08.2025)

Abstract: The paper presents a refined approach for integrating a solar power system and supercapacitor energy storage system into the urban railway traction power supply system. The primary aim is to optimize the use of renewable energy by efficiently utilizing solar power to meet traction power demands, thereby reducing the dependence on energy from traction transformers. The proposed solution involves utilizing a combination of Newton's method with a dynamic programming algorithm. The dynamic programming algorithm determines the optimal energy distribution strategy among supercapacitors, solar panels, and traction transformers to minimize the objective function for each supercapacitor capacity and solar power rating. Newton's method estimates the optimal supercapacitor value to achieve the minimum objective function. The proposed method is validated through a simulation model developed in MATLAB using data from the Cat Linh-Ha Dong urban railway line. The results demonstrate a 65.56% reduction in energy supplied from the grid, and further reductions are achievable in areas with higher radiation levels or expanded solar panel deployment along the railway line.

Key words: clean energy railway transportation, low carbon emission, optimal algorithm, photovoltaic energy, supercapacitor energy storage system

1. Introduction

In the current scenario of the Earth experiencing an unpredictable rate of warming, attributed mainly to global CO_2 emissions from fossil fuels [1], nations worldwide are increasingly committed to achieving carbon neutrality by 2050. Mitigating CO_2 emissions is a pervasive focus across

various sectors, particularly in energy [2]. The domain of electric railway transportation, which does not directly produce CO_2 emissions, relies on a substantial electricity supply from power plants, indirectly contributing to CO_2 emissions [3]. However, electric railway transportation possesses distinctive features, such as the substantial generation of renewable energy during braking and the potential for seamless integration of other renewable energy sources (such as solar and wind), offering numerous solutions to reduce reliance on power plant-supplied energy [4, 5].

The recuperation of regenerative braking energy in urban railway systems is crucial for sustainability and efficiency. Research suggests that as much as 53% of the total energy consumed in urban railways can be traced back to renewable sources during operational transitions. After factoring in drag and mechanical movement losses, 22% to 40% of the energy consumption is projected to be reclaimed through electrical regeneration [6]. Substantial research endeavours are currently focused on improving the efficiency and capability of systems in this domain to achieve more significant energy conservation [7–19]. One potential approach involves capturing the energy trains generate during braking phases [8]. Installing energy storage systems (ESSs) to store surplus braking energy and feed it back into the contact line as needed is an effective solution for implementing this approach [9]. Regarding the stationary ESSs implementation, a solution proposed in reference [12] involves analyzing regenerative currents at stations to assess recoverable energy for a year. This analysis is the basis for determining the appropriate supercapacitor capacity capable of efficiently recovering regenerative energy. Meanwhile, Wang [13] presents a methodology for optimizing the location and size of ultra-capacitors to achieve the best energy savings and voltage profile. This approach is based on an enhanced genetic algorithm and was demonstrated in a case study involving a Chinese metro line. The study's outcome revealed an optimized configuration with an average energy-saving rate of 4.88%, a regeneration cancellation rate of 5.45%, and an installation cost of 3.50 million dollars. In another study, Ratniyomchai [14] delved into identifying the most appropriate capacities and locations for storage devices to minimize the electrical energy consumption of trains and overall line losses. Results confirmed that minimal capacitances were achieved when supercapacitors were positioned near the substations for each electrified line section. Additionally, Xia [15] proposed a novel optimization method combining genetic algorithms and an urban rail power supply system simulation platform, aiming to derive the best energy management strategy, location, and size for Energy Storage Systems (ESSs) concurrently. This study focuses on the simultaneous optimization of energy management, location, and size of stationary super-capacitor ESSs to achieve the best economic efficiency and voltage profile for metro systems. Calderaro [10, 11] explored the design of stationary ESSs based on supercapacitors for metro networks, presenting a heuristic method for jointly determining the siting and sizing of stationary supercapacitors. These studies introduced a new formulation for optimizing ESS siting and sizing, which was addressed using the particle swarm algorithm. Recent research has also focused on developing new methods and formulations to enhance accuracy and efficiency in solving the problem of determining the optimal installation configuration of supercapacitors. Lamedica [16] designed software using the PSO algorithm, with the objective function based on the net present value. David [13] also proposed a model that applies nature-inspired optimization algorithms in combination with a realistic railway simulator.

Several studies have addressed integrating distributed renewable energy sources into the traction power supply system [20–36]. Flavio [21] employed a stochastic optimization method to assess the integration of a solar panel system with a supercapacitor energy storage system

into the railway power system, affirming its feasibility and economic efficiency. Meanwhile, Chu and colleagues [22] proposed a small-signal impedance model to analyze issues related to integrating renewable energy sources into the DC railway power supply network. Another study [23] made recommendations regarding the optimal space and installation location for solar panels, emphasizing the effectiveness of utilizing spaces such as station canopies, tunnel canopies, both sides of road barriers, and the canopies of adjacent works in bolstering the solar power system's capacity. In a study outlined in reference [25], researchers explored incorporating PV and energy storage systems into traction power supply systems. It was demonstrated that this integration can offset traction voltage and minimize transmission losses on the contact grid, leading to increased energy savings. Furthermore, the combined energy efficiency surpasses the sum of the individual efficiencies achieved when the systems are deployed separately. In another investigation by Binduhewa [28] the potential deployment of solar power systems along urban railway lines to achieve net zero emissions was discussed. A methodology for determining the location and capacity of a pilot solar system on the urban railway network of Sri Lanka was proposed. The findings indicated that the solar power system could meet up to 90% of the energy demand for the railway electrification system through efficient train scheduling. Addressing the objective of integrating solar power into the railway traction power supply system in response to the growing demand for renewable energy sources, the authors constructed a neural network model in reference [37] to predict the power output from the solar panel system. This prediction formed the basis for effective control strategies upon integrating the solar panel system with the railway traction power supply system.

This paper explores integrating solar panels and energy storage systems into the urban railway traction power supply. The objective is to determine the capacity of the storage device and solar panel power output and to develop a control strategy for efficient power distribution from the solar panel, supercapacitor, and traction transformer. The aim is to maximize the utilization of renewable energy sources, minimize grid energy supply, and indirectly reduce CO_2 emissions. The proposed methodology utilizes a combination of dynamic programming algorithm and Newton method. Dynamic programming determines the optimal energy distribution mode, while the Newton iteration method identifies the optimal supercapacitor value to achieve the desired objective function. The effectiveness of the proposed method is validated using a simulation model developed in MATLAB software based on data from the Cat Linh-Ha Dong railway line.

2. Modelling the power system for an urban railway line with integrated solar system and supercapacitor system

The DC power supply system comprises substations, contact lines, trainloads, tracks, and return lines. Traction current originates from the rectified substation and is transmitted through the contact network to the trains. Subsequently, the current travels through the running track and return lines, ultimately returning to the substation. In terms of the electrical circuit model, the substation is represented as a DC supply, while a variable value current source characterizes trains. The contact line and tracks are depicted as distributed resistors.

Trains are conceptualized as current sources that absorb power during traction and generate power during regenerative braking. The power at the wheels is computed for a given speed,

considering the need to overcome vehicle inertia, slopes, curves, aerodynamic friction, and rolling friction. By factoring in the vehicle components and their associated efficiencies, the power required from the contact line is determined as follows:

$$P_{tr}(t) = \begin{cases} \dfrac{F_k(t) \cdot v(t)}{\eta_k} + P_{phu} \\ -F_h(t) \cdot v(t) \cdot \eta_h + P_{phu} \end{cases}, \tag{1}$$

where:

$v(t)$ – train speed is determined according to the speed profile.

$F_k(t)$ – traction force that is determined relative to the operating speed from the speed-traction force characteristic.

$F_h(t)$ – braking force is determined relative to the operating speed from the speed-braking force characteristic.

η_k – efficiency in traction mode, which includes the efficiency of the gearbox, the motor, and the inverter.

η_h – efficiency in braking mode.

P_{phu} – the power required for accessories services.

After calculating the train's power requirements for the route, we can determine the traction load power ($P_{\text{sub\_load}}$) needed for the traction substations based on the different operating modes of the railway line. This allows us to calculate the required load current for the traction substations:

$$I_{dmd} = \frac{P_{\text{sub\_load}}}{V_{\text{sub}}}. \tag{2}$$

Substations are modelled as ideal voltage sources (E_{sub}) with a series resistance (R_{ng}).

The supercapacitor module is connected to the traction system utilizing a bi-directional DC-DC converter in the energy storage system. However, a supercapacitor energy storage system can be simplified and modelled by a capacitor in series with a resistor (R_{SC}). The model equation of the supercapacitor module can be expressed as follows:

$$\begin{gathered} R_{\text{SC}} I_{\text{SC}} + V_{\text{SC}} + V_{\text{sub}} = 0, \\ I_{\text{sc}} = C_{\text{SC}} \frac{\mathrm{d}V_{\text{SC}}}{\mathrm{d}t}, \\ E_{\text{SC}}(t) = \int_0^T P_{\text{SC}}(t)\mathrm{d}t = \int_0^T V_{\text{SC}}(t) \cdot I_{\text{SC}}(t)\mathrm{d}t = \frac{1}{2} C_{\text{SC}} \int_0^T V_{\text{SC}}^2(t)\mathrm{d}t. \end{gathered} \tag{3}$$

The supercapacitor voltage and current are $V_{\text{SC}}(t)$ and $I_{\text{SC}}(t)$, respectively.

The solar cell model is composed of a current source (J_{pv}), a shunt resistance (R_{sh}) and a series resistance (R_s). The characteristic equation of solar cell is given by:

$$\begin{gathered} I_{\text{pv}} = J_{\text{pv}} - I_{\text{sh}}, \\ v_{\text{sub}} = J_{\text{pv}} R_{\text{sh}} - I_{\text{pv}} R_s \\ I_{\text{pv}} = \frac{P_{\text{pv}}}{v_{\text{sub}}}. \end{gathered} \tag{4}$$

The contact lines and tracks are represented as electrical resistances. As trains travel between successive stations or substations, the electrical resistance between the train and the initial substation, and between the train and the next substation, varies with time. Consequently, at each time interval, the resistance of a particular section between two trains and between the train and the substation is computed as follows:

$$\begin{aligned} R_{1-2} &= R_0 \times |x_1 - x_2|\,, \\ R_{\text{sst}-2} &= R_{ng} + R_0 \times |x_{\text{sst}} - x_2|\,, \end{aligned} \tag{5}$$

where R_0 is the resistance of the contact line and track per one km; then x_1 and x_2 are the location of two subsequent trains; x_{sst} is the location of the substation; R_{ng} is the resistance of the feeder.

Figure 1 shows a model of a typical urban train network with integrated stationary ESSs and a Photovoltaic system.

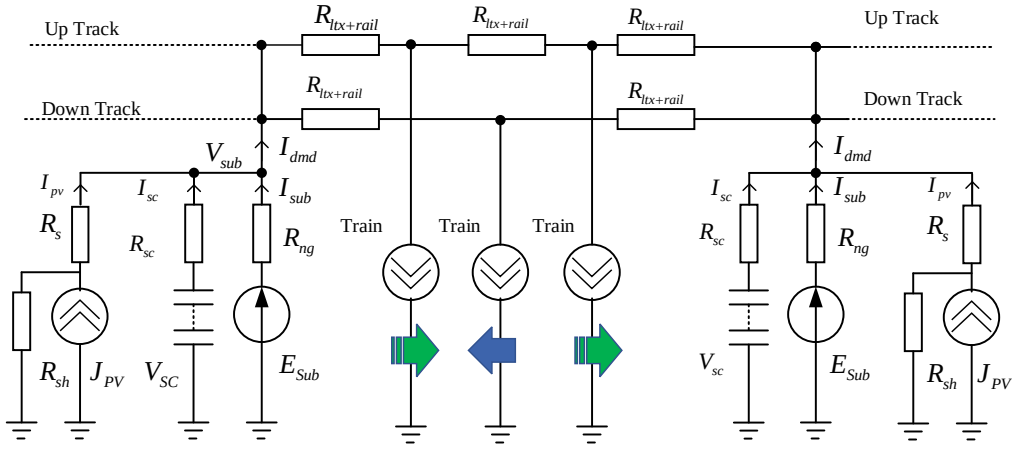

Fig. 1. Urban railway line model with the supercapacitor storage system and PV system

3. Optimization method

3.1. Problem formulation

To identify the best supercapacitor current parameter throughout the entire cycle, we can utilize the dynamic programming algorithm to optimize the energy distribution process at each time point. The system model for determining the control parameters can be found in Eq. (6), as inferred from the circuit diagram in Fig. 1.

$$\begin{cases} I_{\text{sub}} + I_{\text{sc}} + I_{\text{pv}} - I_{dmd} = 0 \\ I_{\text{sc}} = C\dfrac{\mathrm{d}V_{\text{sc}}}{\mathrm{d}t} \\ I_{\text{pv}} = \dfrac{P_{\text{pv}}}{V_{\text{sub}}} \quad I_{dmd} = \dfrac{P_{\text{sub\_load}}}{V_{\text{sub}}} \\ V_{\text{sub}} = V_{\text{sc}} + R_{\text{sc}} C\dfrac{\mathrm{d}V_{\text{sc}}}{\mathrm{d}t} \end{cases} . \tag{6}$$

The objective is to optimize the power supply's energy usage from the traction transformer-rectifier by effectively utilizing the energy stored in the supercapacitor and solar cell to fulfil the load requirements. Simultaneously, the aim is to efficiently capture and store all regenerative braking energy from the train and the surplus electricity generated by the solar cell to minimize voltage fluctuations and reduce energy dissipation on the braking resistor. The goal is achieved by defining the objective function in expression (7):

$$FC = \min E_{\text{sub}} = \min \int_{t=4h45}^{t=22h45} P_{\text{sub}}(t)\mathrm{d}t = \min \int_{t=4h45}^{t=22h45} V_{\text{sub}}(t) \times I_{\text{sub}}(t)\mathrm{d}t. \tag{7}$$

During the evaluation cycle lasting from 4:45 to 22:45, E_{sub} denotes the traction power supplied by the transformer-rectifier, V_{sub} and I_{sub} represent the voltage and current after being rectified.

To achieve the objective above, two selected control variables are the supercapacitor current (I_{sc}) and the PV current I_{pv} (or the current of the DC/DC converter). $P_{\text{sub\_load}}$ or I_{dmd} is chosen as input variable. Additionally, the rectified current from the traction transformer (I_{sub}) and the voltage across the supercapacitor (V_{sc}) are designated as the state variables of the system.

For the optimization process, the initial conditions of the state parameters are assumed: $I_{\text{sub}}(0) = 0$; $V_{\text{sc}}(0) = 0 \div 20\% V_{\text{sc\_max}}$.

The constraints for the optimal parameter set are required:

$$\begin{gathered} 0 \le I_{\text{sub}} \le I_{dmd} \\ 0 \le I_{\text{pv}} \le I_{pv_{\max}} \\ I_{\text{sc\_min}} \le I_{\text{sc}} \le I_{\text{sc\_max}} \\ V_{\text{sc\_min}} \le V_{\text{sc}} \le V_{\text{sc\_max}} \end{gathered} . \tag{8}$$

Based on the chosen control and state variables, along with the constraints outlined in Formula (8), utilizing the dynamic programming algorithm to maximize the objective function (7) for model (6) will enable the identification of the best control approach for the discharge/charge state of the supercapacitor, as well as the optimum control strategy for power supply from the PV module. This will determine the most efficient energy distribution mode in the traction power station system that integrates supercapacitor storage and solar power sources.

3.2. Optimal algorithm

The proposed optimization method involves the integration of two algorithms: the dynamic programming algorithm and the Newton method. The Newton method calculates the traction load of each station at every point during the operational cycle. This is the foundation for determining the load demand and estimating renewable energy. Additionally, the Newton method is applied to identify the optimal value of the supercapacitor to maximize the recovery of regenerative energy and surplus energy generated by the solar cell. The dynamic programming algorithm is then employed to minimize the objective function corresponding to the supercapacitor values and the rated power generated by the solar cell.

Figure 2 presents the flow chart of the proposed algorithm.

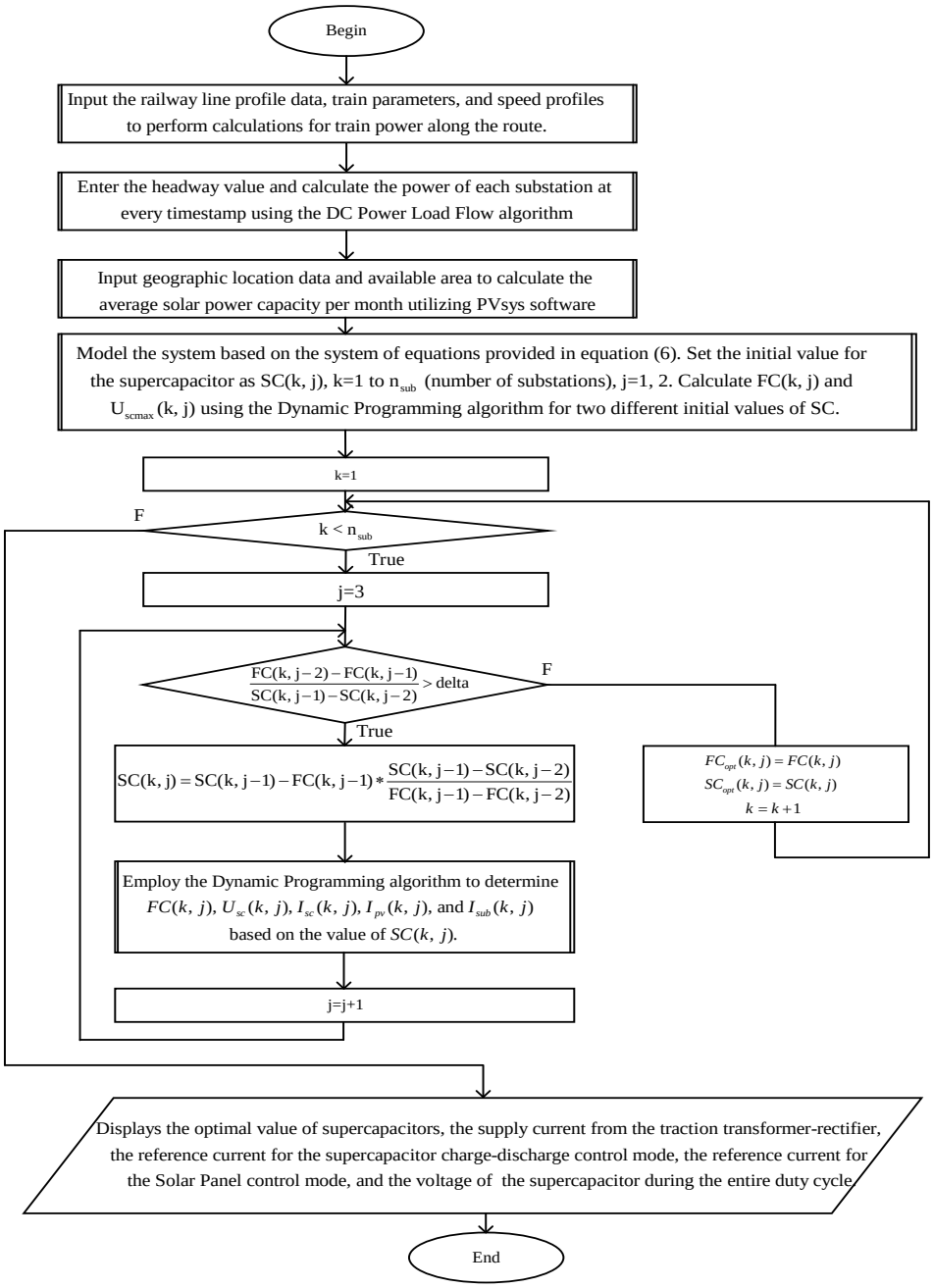

Fig. 2. Flow chart of the proposed algorithm

The procedure of the proposed algorithm is presented as follows:

Step 1. Determine the power of a train at each time point along the route.

This step calculates the power of a train according to the time when moving along the railway line from the initial station to the final station in one direction. This power is specified according to Eq. (1). If the traction (braking)-speed characteristics are unavailable, conventional methods can be used to determine the traction force based on the route profile, train mass, and speed profile.

Step 2. Determine the traction load capacity at the substations.

In this step, the value of headway must be entered, and then an algorithm is implemented to construct the traction power circuit topology at each point in the operational cycle. This algorithm determines the position and power of each train along the entire line, as well as the configuration of the traction power circuit formed by traction substations, overhead contact lines, and the trains themselves. It also calculates the resistance values of the contact lines and the running rails that connect the traction substation to the train, or between trains. Next, the Newton-Raphson algorithm is applied to determine the power requirements of the traction substation at each corresponding moment according to the traction power circuit topology established by the previous algorithm. Since the traction circuit operates as a direct current (DC) system, the power equation considers only real power, excluding reactive power or phase angle. The traction substations are modeled as slack-bus type. These two algorithms are executed sequentially for each time point within the headway cycle. By the end of this step, the result achieved will be the power requirements of the traction substations at every time point throughout the entire operational cycle.

In addition, the required current of the traction load (I_{dmd}) at each time point in the operating cycle can be calculated from the power and voltage quantities.

Step 3. Determine the solar power capacity that can be supplied.

Based on the information of geographic coordinates, the usable area for solar panels, and the installation plan, the PVsyst software is then applied to estimate the level of electricity generated from solar energy to supply the traction power system for each hour of the day of each month of the year.

Step 4. Determine the objective function value for the two initial values of the supercapacitor.

In this step, utilize the dynamic programming algorithm to optimize the power distribution mode from the traction transformer, supercapacitor, and solar panel to supply the traction load corresponding to the two initial values for the supercapacitor $\mathrm{SC}(k,1) = 10$ and $\mathrm{SC}(k,2) = 20$. The optimal mode is determined to recover the regenerative braking energy fully, fully utilize the generated solar energy, and minimize voltage fluctuations. From there, the objective function is chosen to minimize the electrical energy supplied from the traction power station.

Step 5. Determine the optimal value of the supercapacitor.

Based on the results obtained in step 4 with two initial values. In step 5, the Newton method is applied to determine the approximate value of the supercapacitor through iterations to converge to the minimum objective function value as quickly as possible. Since the objective function in expression (7) has a nonlinear and implicit relationship with the values of the supercapacitor, as described by the system equations in expression (6), this study employs a dynamic programming algorithm to determine the objective function values associated with each supercapacitor value. The system model, state variables, control variables, and constraint conditions are outlined in Section 3.1. A single execution of the algorithm will produce the objective function value, as well as sets of state variable values and control variable values, which include the current and voltage of the solar module. This process enables the determination of the PV's capacity.

At the end of step 5, the optimal capacity of the supercapacitor installed at each substation is determined to minimize the energy supplied by the traction transformer. Additionally, the current and voltage of the solar battery are assessed, allowing for an estimation of the required capacity from the photovoltaic (PV) system. Simultaneously, the best control strategy for energy storage is identified, which includes the charge and discharge processes for both the supercapacitor and the solar cells.

Step 6. Display the results.

Displays the algorithm execution results, including the optimal value of the supercapacitor, the supply current from the traction transformer-rectifier, the reference current for the supercapacitor charge-discharge control mode, the reference current for the Solar Panel control mode, and the voltage of the supercapacitor during the entire duty cycle.

Step 7. End

4. Simulation results

4.1. Case study

To experiment with the proposed solution, simulations on a model of an urban railway line were carried out in MATLAB. The information of the simulating model is referred to in [38, 39]. This railway line has a total length of 12.6 km, on which there are 12 stations (Cat Linh, La Thanh, Thai Ha, Lang, Thuong Dinh, Vanh Dai 3, Phung Khoang, Van Quan, Ha Dong, La Khe, Van Khe, Yen Nghia), and it is powered by 6 substations (Cat Linh, Lang, Vanh Dai 3, Van Quan, La Khe, Yen Nghia) – see Fig. 3. Table 1 shows the leading electrical and topological characteristics of this line, as well as the information regarding the rolling stock.

Table 1. The main electrical and topological characteristics

Parameters	Value
Line length	12.6 km
Station location	0; 0.93; 1.81; 2.89; 4.14; 5.15; 6.45; 7.75; 9.08; 10.18; 11.62; 12.60
Substation location	0; 2.89; 5.15; 7.75; 10.18; 12.60
Nominal voltage	750 VDC
Train mass	145 ton
Auxiliary power	200 kW
Maximum speed	80 km/h
Headway	360 seconds for times from 7:00–8:30 and 17:00–18:30 600 seconds for the remaining times
Resistance per unit of contact line and track	0.065 Ω/km
Resistance of feeder	0.01 Ω

Table 2 describes the travel time of trains between stations and the whole route. Assume that the departure time from the first station is 0 seconds, and the rest time at the stations is assumed to be 30 seconds. The total time for the journey from the first station to the last station is 1 292 seconds (about 21.5 minutes). The journey in the opposite direction took 1 285 seconds.

Fig. 3. Map of stations in the Cat Linh-Ha Dong railway line

Table 2. The journey time of the train along the railway line

Departure station	Arrival station	Departure time (second)	Arrival time (second)	Journey time (second)	Rest time (second)
1	2	0	88	88	30
2	3	118	196	78	30
3	4	226	317	91	30
4	5	347	450	103	30
5	6	480	559	79	30
6	7	589	693	104	30
7	8	723	809	86	30
8	9	839	936	97	30
9	10	966	1050	84	30
10	11	1080	1181	101	30
11	12	1211	1292	81	30
12	11	1292	1372	80	30
11	10	1402	1503	101	30
10	9	1533	1617	84	30
9	8	1647	1744	97	30
8	7	1774	1859	85	30
7	6	1889	1995	106	30
6	5	2025	2103	78	30
5	4	2133	2237	104	30
4	3	2267	2355	88	30
3	2	2385	2464	79	30
2	1	2494	2577	83	30

The railway line surveyed in this case study is located at the coordinates (Latitude: 20.9923, Longitude: 105.8044, Altitude: 29 m above sea level, Locality: Thanh Xuan, Country: Vietnam) as illustrated on the map with an effective area for deploying the Solar Panel system at each station of about 6377 m^2. Based on the PVsyst software tool, the average hourly electricity generation capacity during the days of the month of the year is estimated in Table 3.

Table 3. The average hourly electrical power for each month generated from the solar system on the 377 m^2 area of the substation roof [kW]

	Jan	**Feb**	**Mar**	**Apr**	**May**	**Jun**	**Jul**	**Aug**	**Sep**	**Oct**	**Nov**	**Dec**
0 h	0	0	0	0	0	0	0	0	0	0	0	0
1 h	0	0	0	0	0	0	0	0	0	0	0	0
2 h	0	0	0	0	0	0	0	0	0	0	0	0
3 h	0	0	0	0	0	0	0	0	0	0	0	0
4 h	0	0	0	0	0	0	0	0	0	0	0	0
5 h	0	0	0	0	0	0	0	0	0	0	0	0
6 h	0	0	4	48	74	81	74	41	51	38	1	0
7 h	27	37	94	160	222	244	242	178	193	145	40	34
8 h	81	102	243	282	354	380	395	304	339	262	94	84
9 h	125	171	346	391	454	494	510	423	437	354	147	131
10 h	154	231	388	483	510	571	584	496	512	417	187	163
11 h	174	264	440	529	533	570	579	531	528	449	186	177
12 h	163	264	409	518	519	565	592	527	538	431	172	161
13 h	153	282	361	509	505	542	554	470	511	382	145	193
14 h	115	245	304	393	423	484	476	393	424	304	115	146
15 h	69	175	207	280	318	363	364	313	301	190	64	92
16 h	28	82	113	151	179	220	231	186	157	74	23	33
17 h	0	2	26	32	47	67	81	46	15	0	0	0
18 h	0	0	0	0	0	0	0	0	0	0	0	0
19 h	0	0	0	0	0	0	0	0	0	0	0	0
20 h	0	0	0	0	0	0	0	0	0	0	0	0
21 h	0	0	0	0	0	0	0	0	0	0	0	0
22 h	0	0	0	0	0	0	0	0	0	0	0	0
23 h	0	0	0	0	0	0	0	0	0	0	0	0

4.2. Numerical results

Based on the main electrical and topological characteristics described in Table 1 and the journey time of the train moving along the railway line, as shown in Table 2, the train power at each time is estimated. To calculate the power according to Formula (1), the traction force and speed values are calculated according to the empirical method mentioned in the reference [40]. Figure 4 illustrates the power-time graph of the train travelling along the route. Power is positive and increases with acceleration. This value decreases slightly when the train operates at a constant speed. In the braking phases, the power will be negative. And the time when trains stop at the stations, the power will be zero.

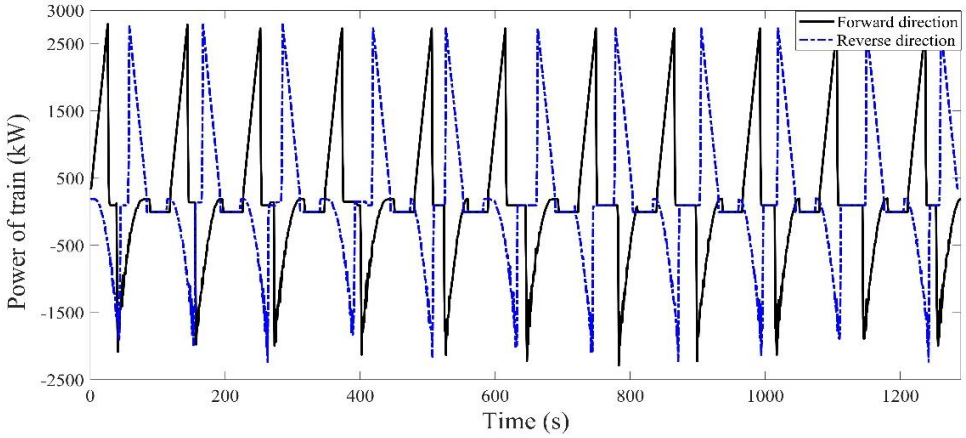

Fig. 4. The power of the train at each time point along the railway line

In the case study, the headway value is selected to be 360 (s) during the operating time from 7:00 to 8:30 and from 17:00 to 18:30, and in the remaining time periods, it is equal to 600. Apply the power flow algorithm as developed in the reference [32] to determine the power value of substations at various times in the headway duration. Figure 5 illustrates the power-time graph of the substations.

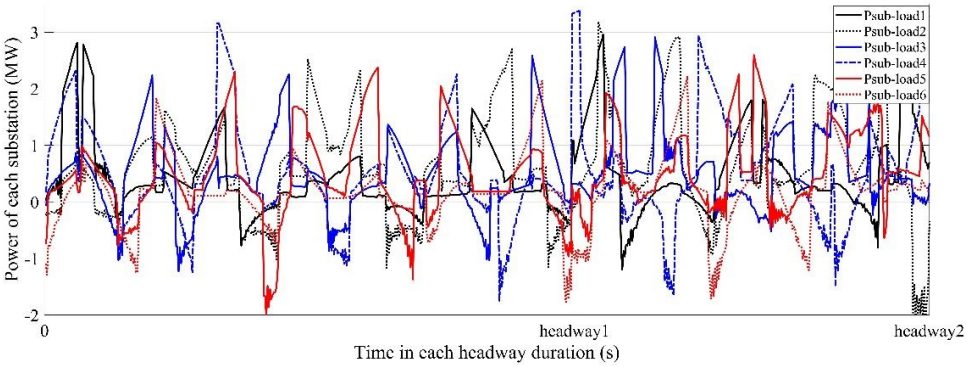

Fig. 5. Power of the substations at each time point

The solar power capacity that can be supplied to the selected station is the average value for 12 months in a year, calculated from the data in Table 3.

Utilizing the proposed algorithm by the aforementioned data, the outcomes are articulated in Fig. 6 and Table 4.

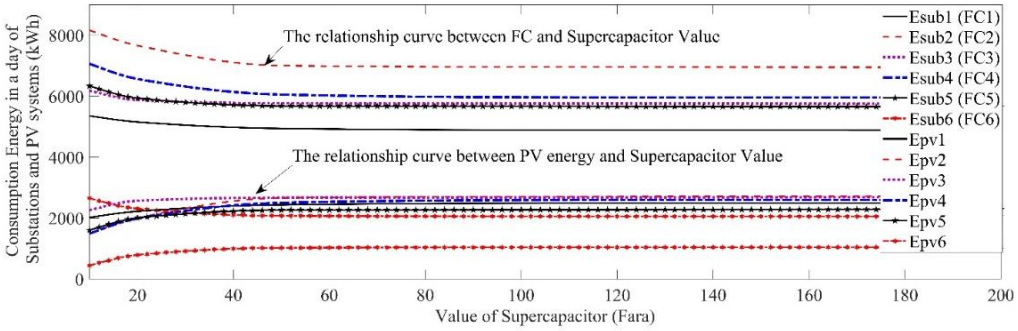

Fig. 6. Optimal value of function cost (Eq. 7) according to supercapacitor value

Table 4. Proposed algorithm execution results for substations

Location	C_{SC} **(F)**	V_{SCmax} **(Volt)**	E_{SCmax} **(kWh)**	E_{pV} **(kWh)**	E_{sub} **(kWh)**
Substation1 (Cat Linh)	48	787	4.13	2431.4	4 944.6
Substation2 (Lang)	50	807	4.52	2663	7003
Substation3 (Vanh Dai3)	38	817	3.52	2661.8	5 780.6
Substation4 (Van Quan)	62	793	5.42	2557.2	5 999.2
Substation5 (La Khe)	46	810	4.2	2259.2	5 680.9
Substation6 (Yen Nghia)	46	802	4.1	1023	2 075.6

This includes the determination of the optimal supercapacitor values for each traction power station, as well as the maximum operational voltage of the supercapacitor. Consequently, this aids in establishing the requisite capacity of the supercapacitor energy storage system for the substation. Additionally, the algorithm's implementation results unambiguously identify the power supplied by the Solar Panel system at each instance, thereby facilitating the determination of the solar panel system's capacity rating and the compatible energy conversion equipment within the system.

The algorithmic results are instrumental in determining the reference current for the optimal control mode of the supercapacitor energy storage and charge-discharge process and the solar cell module. Figure 7 illustrates the currents of the supercapacitor and the photovoltaic cell, in addition to the currents from the traction power station and the current required from the traction load. A relatively small-time frame of approximately 700 seconds is chosen for ease of observation. Upon observing the correlation values of the current quantities, it becomes apparent that the current from the traction transformer only supplies the load when the energy from the solar cell and the supercapacitor is insufficient to meet the load's requirements. Instances, where the load current displays a negative value, signify substantial regenerative energy produced by the train braking, which is then absorbed and stored in the supercapacitor to minimize energy wastage and prevent an increase in the contact grid voltage. Furthermore, when the traction load exhibits a small or negative value, the energy generated from the solar panel can supply excess power to the traction load, which is likewise absorbed and stored in the supercapacitor. The determined I_{sc} and I_{pv} currents will serve as reference currents for executing the optimal control algorithm for the corresponding power converters in the system.

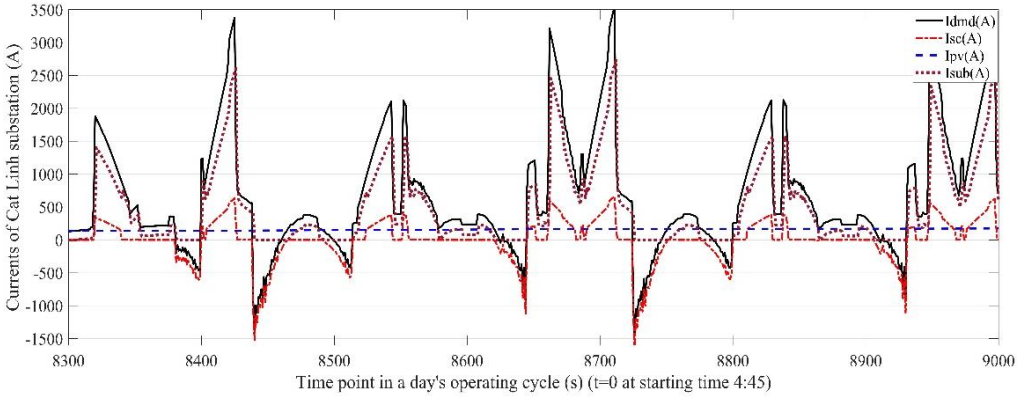

Fig. 7. Currents of the Cat Linh Substations at each time point from 8 300 to 9 000

The diagram in Fig. 8 provides a detailed depiction of the supercapacitor's charging and discharging processes throughout a typical daily working cycle, spanning from 4:45 to 22:40. During the initial phase of the day, from 4:45 to approximately 8:00, before the solar panel generating electricity, the supercapacitor's energy fluctuates under the storing and subsequent discharging of regenerative energy, combined with the transformer's energy to meet the load demand. From 8:00 until around 15:00, as solar energy production gradually increases, the supercapacitor also accumulates surplus energy from the solar panel, resulting in a corresponding uptick in stored energy levels. Subsequently, post 15:00, as solar energy production diminishes, the supercapacitor's energy levels also tend to decrease. Analysis of the energy curve for station number 3 (Escsub3 – VD3 Substation) reveals a peak value of approximately 3.52 kWh, the lowest among the stations, signifying comparatively limited renewable energy recoverable at this location. Additionally, the energy stored in the supercapacitor declines to near the early-day levels around 17:00, indicating substantial capacity to absorb additional solar energy. In contrast, station number 6 (Escsub6 – Yen Nghia Substation) displays a gradual increase in the supercapacitor energy

curve, reaching its peak around 17:00, indicative of relatively abundant renewable energy at this location. The energy stored in the supercapacitor from the solar panels and renewable energy is then released throughout the latter part of the day, extending beyond 22:00, highlighting the approaching of the solar panel's energy absorption limit at this location.

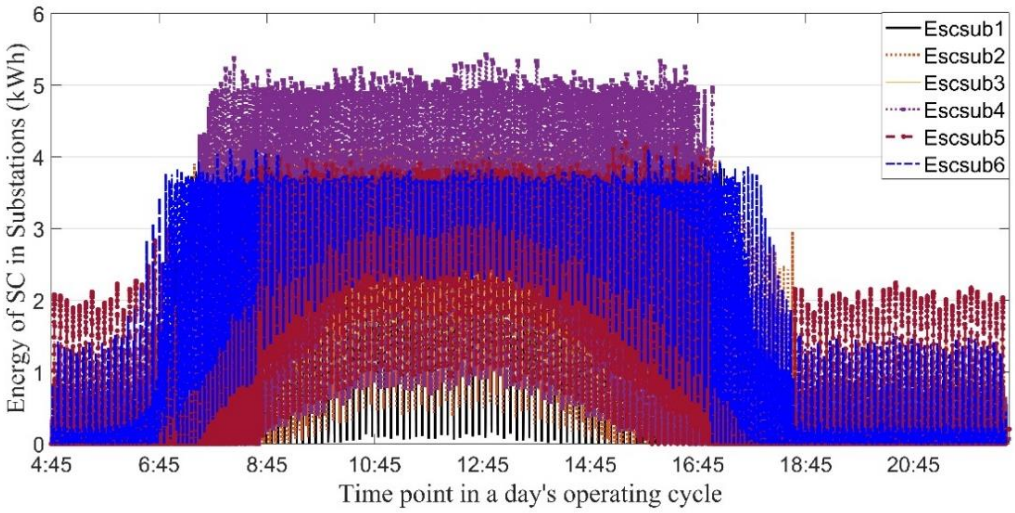

Fig. 8. Energy of supercapacitor in substations

Figure 9 compares the power supply from the traction transformer of the stations with and without the integration of the solar panel system and the supercapacitor energy storage system. Among the stations, station No. 1 (CatLinh Substation) showed the least reduction, with the power supplied by the traction transformer decreasing to 59.93% after the integration. On the other hand, station No. 6 (Yen Nghia Substation) exhibited the most significant reduction, with the power consumption from the traction transformer dropping to only 39.4% after implementing the solar panel and supercapacitor system. The remaining stations saw an average reduction in energy of about 56–58%.

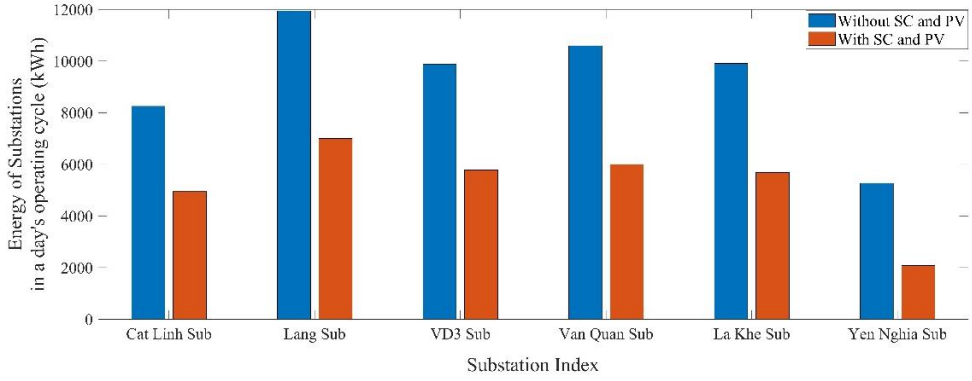

Fig. 9. Energy consumption of substations with and without SC, PV

If the economic considerations are disregarded, it is possible to sufficiently increase the capacity of the supercapacitor to fully recover the renewable energy generated from regenerative braking and solar power. In this case, the optimal outcome is achieved, as presented in Table 5, with the energy savings associated with each substation outlined in Figure 10.

Table 5. Proposed algorithm execution results for maximum recovery and utilization of renewable energy

Location	C_{SC} **(F)**	V_{SCmax} **(Volt)**	E_{SCmax} **(kWh)**	E_{pV} **(kWh)**	E_{sub} **(kWh)**
Substation 1 (Cat Linh)	7 142	746.6	552.98	3 278.9	2 713.6
Substation 2 (Lang)	3 334	671.2	208.55	3 677	5 006.2
Substation 3 (Vanh Dai3)	5 556	702.3	380.63	3 613.1	3 806.3
Substation 4 (Van Quan)	5 390	750	421.14	3 638.2	3 918.9
Substation 5 (La Khe)	6 250	746.2	483.42	3 528.8	3 310.2
Substation 6 (Yen Nghia)	7 500	622.4	403.52	2 541.6	473.6

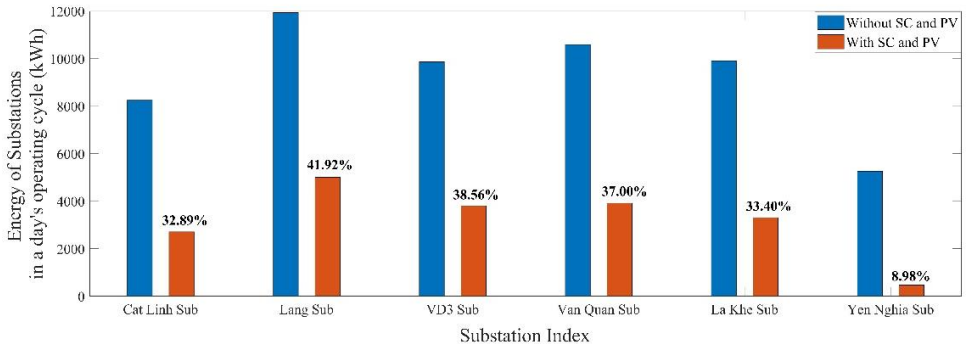

Fig. 10. Energy consumption of substations with and without SC, PV

Among the substations under consideration, Substation No. 2 (Lang Substation) demonstrated the smallest reduction, with the power supplied by the traction transformer decreasing to 41.92% following the integration. In contrast, Substation No. 6 (Yen Nghia Substation) exhibited the most significant reduction, with the power consumption from the traction transformer dropping to only 8.98% after the implementation of the solar panel and supercapacitor system. The remaining substations saw an average reduction in energy of about 34.44%. Under these conditions, the energy consumption could be reduced by up to 65.56%. Notably, except for station No. 6, the other stations

can receive additional energy from the solar panel. Expanding the solar panel installation area, including along the road barrier and between the rails, could significantly increase energy production from the solar panels, further reducing energy consumption from the traction transformer.

The data above presents the outcomes of testing the proposed approach for the Cat Linh-Ha Dong railway model. The route is situated in an area with moderate solar radiation, averaging about 1 000 hours of sunshine annually. By comparing the energy consumption of the traction power supply system before and after integrating the solar energy system and the supercapacitor energy storage system, we can evaluate the solution's potential and effectiveness in urban railway electric transport. This evaluation is essential as we strive to achieve the goal of achieving zero CO_2 emissions by 2050.

5. Conclusions

The paper outlines a method for optimizing the capacity of supercapacitors and the peak power of solar panels while also determining the best energy distribution strategy between supercapacitors, solar panels, and traction transformers for supplying traction loads. The goal is to integrate solar and supercapacitor energy storage systems into the traction power supply system to minimize grid energy usage and indirectly reduce CO_2 emissions. The proposed optimization method has been tested on the Cat Linh-Ha Dong line data model, resulting in a 43.61% reduction in energy consumption. Furthermore, the energy consumption could be reduced by up to 65.56% with the maximization of the supercapacitor's capacity. This outcome serves as a basis for potential implementation on specific railway lines.

References

[1] Dongyang Zhang, Yumei Guo, Farhad Taghizadeh-Hesary, *Green finance and energy transition to achieve net-zero emission target*, Energy Economics, vol. 126, 106936 (2023), DOI: 10.1016/j.eneco.2023.106936.

[2] Tsvetkov Pavel, Samuseva Polina, *Heterogeneity of the impact of energy production and consumption on national greenhouse gas emissions*, Journal of Cleaner Production, vol. 434, no. 1, 139638 (2024), DOI: 10.1016/j.jclepro.2023.139638.

[3] Nakaret Kano, Zhongbei Tian, Nutthaka Chinomi, Xiaoguang Wei, Stuart Hillmansen, *Renewable Sources and Energy Storage Optimization to Minimize the Global Costs of Railways*, IEEE Transactions on Vehicular Technology, vol. 74, iss. 5, pp. 1–11 (2023), DOI: 10.1109/TVT.2023.3265944.

[4] Aleksy Kwilinski, Oleksii Lyulyov, Tetyana Pimonenko, *Reducing transport sector CO2 emissions patterns: Environmental technologies and renewable energy*, Journal of Open Innovation: Technology, Market, and Complexity, vol. 10, no. 1, 100217 (2024), DOI: 10.1016/j.joitmc.2024.100217.

[5] Zhanhe Li, Xiaoqian Li, Chao Lu, Kechun Ma, Weihan Bao, *Carbon emission responsibility accounting in renewable energy-integrated DC traction power systems*, Applied Energy, vol. 355, no. 1, 122191 (2024), DOI: 10.1016/j.apenergy.2023.122191.

[6] Hui-Jen Chuang, *Optimization of inverter placement for mass rapid transit systems by immune algorithm*, Electric Power Applications (IEE Proc Elec Power Appl), of Conference, IEEE (2005), DOI: 10.1049/ip-epa:20041143.

[7] José Antonio Aguado, Antonio José Sánchez Racero, Sebastián de la Torre, *Optimal Operation of Electric Railways with Renewable Energy and Electric Storage Systems*, IEEE Transactions on Smart Grid, vol. 9, no. 2, pp. 993–1001 (2018), DOI: 10.1109/TSG.2016.2574200.

[8] Spalvieri C., Rossetta I., Lamedica R., Ruvio A., Papalini A., *Train braking impact on energy recovery: the case of the 3 kV d.c. railway line Roma-Napoli via Formia*, 2019 AEIT International Annual Conference (AEIT), IEEE, Florence, Italy (2019), DOI: 10.23919/AEIT.2019.8893399.

[9] Mihaela Popescu, Alexandru Bitoleanu, *A Review of the Energy Efficiency Improvement in DC Railway Systems*, Energies, vol. 12, no. 6, pp. 1092–1117 (2019), DOI: 10.3390/en12061092.

[10] Vito Calderaro, Vincenzo Galdi, Giuseppe Graber, Antonio Piccolo, *Optimal siting and sizing of stationary supercapacitors in a metro network using PSO*, in IEEE International Conference on Industrial Technology (ICIT), IEEE, Seville, Spain (2015).

[11] Vito Calderaro, Vincenzo Galdi, Giuseppe Graber, *Siting and sizing of stationary SuperCapacitors in a Metro Network*, in *AEIT Annual Conference*, IEEE (2013).

[12] Reza Teymourfar, Razieh Nejati Fard, Behzad Asaei, Hossein Iman-Eini, *Energy recovery in a metro network using stationary supercapacitors*, in 2nd Power Electronics, Drive Systems and Technologies Conference, IEEE, Tehran, Iran (2011).

[13] Bin Wang, Zhongping Yang, Fei Lin, Wei Zhao, *An Improved Genetic Algorithm for Optimal Stationary Energy Storage System Locating and Sizing*, Energies, vol. 7, no. 10, pp. 6434–6458 (2014), DOI: 10.3390/en7106434.

[14] Tosaphol Ratniyomchai, Stuart Hillmansen, Pietro Tricoli, *Optimal capacity and positioning of stationary supercapacitors for light rail vehicle systems*, International Symposium on Power Electronics, Electrical Drives, Automation and Motion, IEEE, Ischia, Italy (2014).

[15] Huan Xia, Huaixin Chen, Zhongping Yang, Fei Lin, *Optimal Energy Management, Location and Size for Stationary Energy Storage System in a Metro Line Based on Genetic Algorithm*, Energies, vol. 8, no. 10, pp. 11618–11640 (2015), DOI: 10.3390/en81011618.

[16] Regina Lamedica, Alessandro Ruvio, Laura Palagi, Nicola Mortelliti, *Optimal Siting and Sizing of Wayside Energy Storage Systems in a D.C. Railway Line*, Energies, vol. 13, iss. 23, pp. 6271–6293 (2020), DOI: 10.3390/en13236271.

[17] David Roch-Dupréa, Tad Gonsalvesb, Asunción P. Cucalaa, Ramón R. Pecharromána, Álvaro J. López-Lópeza, Antonio Fernández-Cardador, *Determining the optimum installation of energy storage systems in railway electrical infrastructures by means of swarm and evolutionary optimization algorithms*, Electrical Power and Energy Systems, vol. 124, no. 2, pp. 1–15 (2020), DOI: 10.1016/j.ijepes.2020.106295.

[18] Mariam Saeed, Fernando Briz, Juan Manuel Guerrero, Igor Larrazabal, David Ortega, Victor Lopez, Juan Jose Valera, *Onboard Energy Storage Systems for Railway: Present and Trends*, IEEE Open Journal of Industry Applications, vol. 4, pp. 238–259 (2023), DOI: 10.1109/OJIA.2023.3293059.

[19] Hamed Jafari Kaleybar, Mostafa Golnargesi, Morris Brenna, Dario Zaninelli, *Hybrid Energy Storage System Taking Advantage of Electric Vehicle Batteries for Recovering Regenerative Braking Energy in Railway Station*, Energies, vol. 16, no. 13, 5117 (2023), DOI: 10.3390/en16135117.

[20] Takeshi Igarashi, Teruhisa Kumano, Hitoshi Hayashiya, Toshiaki Takino, *Efficiency improvement of rooftop photovoltaic system at railway station*, Journal of International Council on Electrical Engineering, vol. 7, no. 1, pp. 41–50 (2017), DOI: 10.1080/22348972.2016.1229917.

[21] Flavio Ciccarelli, Luigi Pio Di Noia, Renato Rizzo, *Integration of Photovoltaic Plants and Supercapacitors in Tramway Power Systems*, Energies, vol. 11, no. 2, 410 (2018), DOI: 10.3390/en11020410.

[22] Xiaojuan Zhu, Haitao Hu, Haidong Tao, Zhengyou He, *Stability Analysis of PV Plant-Tied MVdc Railway Electrification System*, IEEE Transactions on Transportation Electrification, vol. 5, no. 1, pp. 311–323 (2019), DOI: 10.1109/TTE.2019.2900857.

[23] Ibragim M. Asanov, Egor Y. Loktionov, *Possible benefits from PV modules integration in railroad linear structures*, Renewable Energy Focus, vol. 25, pp. 1–3 (2018), DOI: 10.1016/j.ref.2018.02.003.

[24] Luigi Pio Di Noia, Renato Rizzo, *Analysis of Integration of PV Power Plant in Railway Power Systems*, 2019 8th International Conference on Modern Power Systems (MPS), IEEE, Cluj-Napoca, Cluj, Romania (2019), DOI: 10.1109/MPS.2019.8759720.

[25] Xiaojun Shen, Hongyang Wei, Li Wei, *Study of trackside photovoltaic power integration into the traction power system of suburban elevated urban rail transit line*, Applied Energy, vol. 260, no. 3, 114177 (2020), DOI: 10.1016/j.apenergy.2019.114177.

[26] Seunghyun Park, Surender Reddy Salkuti, *Optimal Energy Management of Railroad Electrical Systems with Renewable Energy and Energy Storage Systems*, Sustainability, vol. 11, no. 22, 6293 (2019), DOI: 10.3390/su11226293.

[27] Md. Akibur Rahaman, Md. Mustaque Nadim, *Utilization of Railway Track for Grid Connected PV System*, Journal of Power and Energy Engineering, vol. 8, no. 4, pp. 25–33 (2020), DOI: 10.4236/jpee.2020.84003.

[28] Prabath J. Binduhewa, *Sizing Algorithm for a Photovoltaic System along an Urban Railway Network towards Net Zero Emission*, International Journal of Photoenergy, vol. 2021, no. 5, pp. 1–17 (2021), DOI: 10.1155/2021/5523448.

[29] Feng Ding, Jianping Yang, Zan Zhou, *Economic profits and carbon reduction potential of photovoltaic power generation for China's high-speed railway infrastructure*, Renewable and Sustainable Energy, vol. 178, no. 2023, 113272 (2023), DOI: 10.1016/j.rser.2023.113272.

[30] Md. Sajjad-Ul Islam, Md. Kousar Ahmed, Patwary Rezwan Mahadi, Md. Farhadul Islam, Asiful Islam, Syeda Tanjila Islam Meem, *Solar Panel Integration on Metro Rail Tracks for Sustainable Energy Generation*, 2024 3rd International Conference on Advancement in Electrical and Electronic Engineering (ICAEEE), IEEE, Gazipur, Bangladesh (2024), DOI: 10.1109/ICAEEE62219.2024.10561795.

[31] Bowen Guan, Haobo Yang, Tao Zhang, Xiaohua Liu, Xinke Wang, *Technoeconomic analysis of rooftop PV system in elevated metro station for cost-effective operation and clean electrification*, Renewable Energy Focus, vol. 226, no. 2024, 120305 (2024), DOI: 10.1016/j.renene.2024.120305.

[32] Guannan Li, Siu Wing, *Multi-agent deep reinforcement learning-based multi-time scale energy management of urban rail traction networks with distributed photovoltaic–regenerative braking hybrid energy storage systems*, Journal of Cleaner Production, vol. 466, no. 2024, 142842 (2024), DOI: 10.1016/j.jclepro.2024.142842.

[33] Abdullah Tariq Sipra, Fawad Azeem, Zulfiqar Ali Memon, Sobia Baig, Mujtaba Hussain Jaffery, *Design and assessment of energy management strategy on rail coaches using solar PV and battery storage to reduce diesel fuel consumption*, Energy, vol. 288, no. 1, 129718 (2024), DOI: 10.1016/j.energy.2023.129718.

[34] Yi Huang, Haitao Hu, Yinbo Ge, Haizhu Liao, Jiaming Luo, Shibin Gao, *Joint Sizing Optimization Method of PVs, Hybrid Energy Storage Systems, and Power Flow Controllers for Flexible Traction Substations in Electric Railways*, IEEE Transactions on Sustainable Energy, vol. 15, no. 2, pp. 1210-1223 (2024), DOI: 10.1109/TSTE.2023.3331346.

[35] Pengyu Wei, Muhammad Abid, Humphrey Adun, Desire Kemena Awoh, Dongsheng Cai, Juliana Hj Zaini, Olusola Bamisile, *Progress in Energy Storage Technologies and Methods for Renewable Energy Systems Application*, Applied Sciences, vol. 13, no. 9, 5626 (2023), DOI: h10.3390/app13095626.

[36] Shiwei Xia, Haiyi Wu, Yibo Mao, Ting Wu, Guanghui Song, Jelena Stojkov, *Photovoltaic Power Generation and Energy Storage Capacity Cooperative Planning Method for Rail Transit Self-consistent Energy Systems Considering the Impact of DoD*, IEEE Transactions on Smart Grid, vol. 18, iss. 1, pp. 665–677 (2024), DOI: 10.1109/TSG.2024.3408950.

[37] Lixia Tian, Yuansheng Huang, Shuang Liu, Shize Sun, Jiajia Deng, Hengfeng Zhao, *Application of photovoltaic power generation in rail transit power supply system under the background of energy low carbon transformation*, Alexandria Engineering Journal, vol. 60, no. 6, pp. 5167–5174 (2021), DOI: 10.1016/j.aej.2021.04.008.

[38] Tran Van Khoi, Nguyen Duc Khuong, *Optimal planning of substations on urban railway power supply systems using integer linear programming*, Transport and Communications Science Journal, vol. 70, no. 4, pp. 264–278 (2019), DOI: 10.25073/tcsj.70.4.14.

[39] Chau N.T.M., *Hanoi Urban Railway Project Cat Linh-Ha Dong Line. Package 1: EPC Contact. Technical Design, Book 2: Traffic organization and operation management*, in Railway Project Management Unit, Vietnam Railway Administration (2014).

[40] Tran Van Khoi, An Thi Hoai Thu Anh, Dang Viet Phuc, *Optimizing the urban train speed to minimize the energy consumption and comfort*, Transport and Communications Science Journal, vol. 72, no. 3, pp. 317–329 (2021), DOI: 10.47869/tcsj.72.3.7.